Organic & Biomolecular Chemistry

ROYAL SOCIETY
OF CHEMISTRY
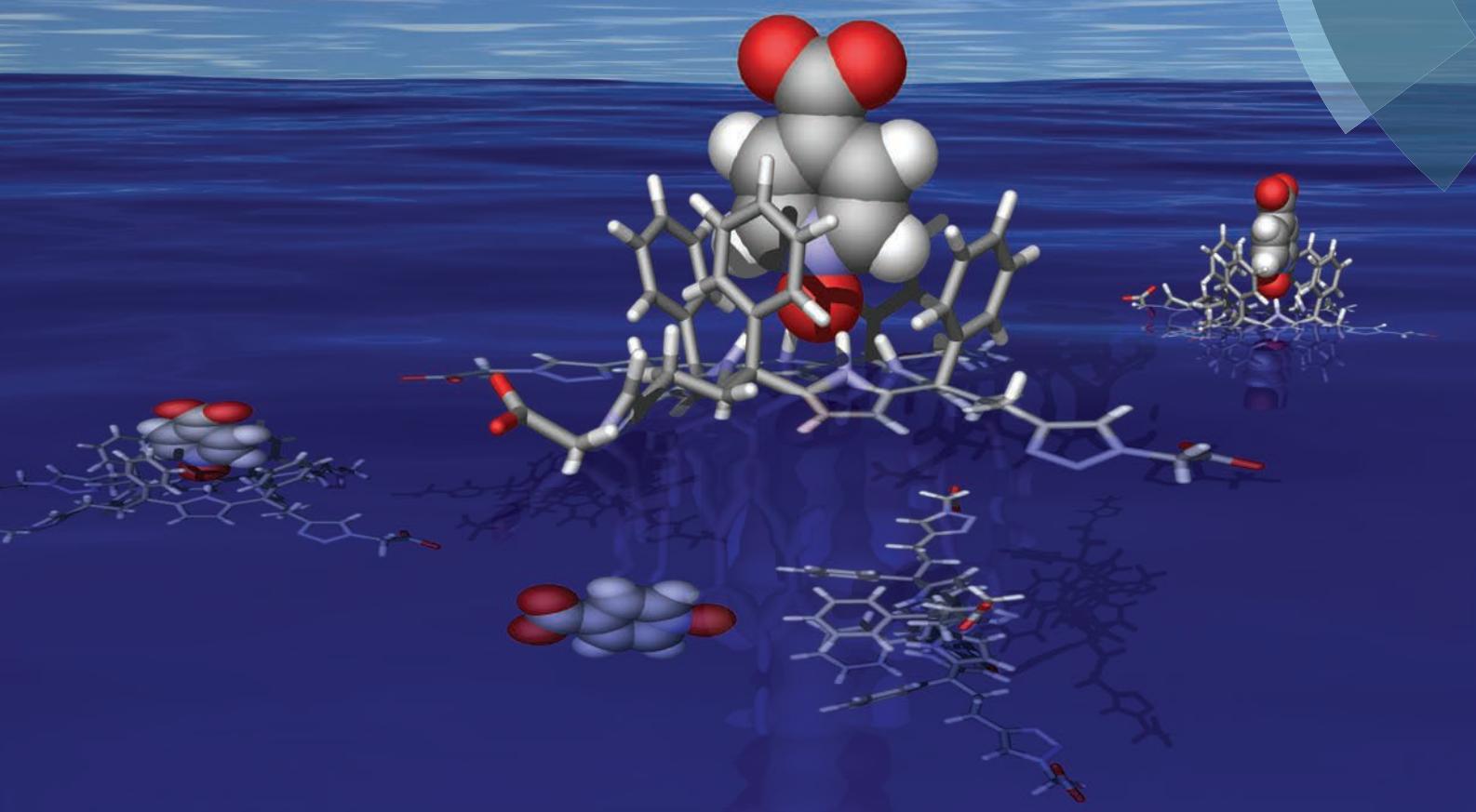
PAPER
P. Ballester et al.
Water-soluble aryl-extended calix[4]pyrroles with unperturbed aromatic
cavities: synthesis and binding studies

PAPER

Water-soluble aryl-extended calix[4]pyrroles with unperturbed aromatic cavities: synthesis and binding studies†

D. Hernández-Alonso,[a] S. Zankowski,[a] L. Adriaenssens[a] and P. Ballester*[a,b]

We report the synthesis of a novel, water-soluble aryl-extended calix[4]pyrrole receptor. The water-solubilising groups are placed at the lower rim of the receptor, leaving the binding pocket unperturbed and open for modification. Binding studies were performed with a series of pyridine *N*-oxides. These studies revealed the ability of the receptor to bind neutral and charged *N*-oxides in basified water with stability constants higher than 10^4 M^{-1}.

Introduction

Calix[4]pyrroles are macrocyclic compounds, consisting of four pyrrole units and four connecting tetra substituted sp[3] carbon atoms, the so-called *meso* carbons.[1,2] Calix[4]pyrroles are well known receptors for anions,[3] ion-pairs[4] and electron rich molecules.[5] Aryl-extended calix[4]pyrroles bear one aryl ring at each *meso* carbon.[6,7] Depending on the relative orientation of these aryl substituents, aryl-extended calix[4]pyrroles exist as four configurational isomers. The α,α,α,α-isomer describes the aryl-extended calix[4]pyrrole with all aryl rings oriented in the same direction, *i.e.* all pointing above the calix[4]pyrrole core (Fig. 1). They are also conformationally flexible and adopt different conformations depending on the media in which they are dissolved.[8] For example, in non-polar organic solvents the least polar 1,3-alternate conformation is the most energetically favourable. Upon the addition of an appropriate hydrogen-bond (H-bond) acceptor to the solution, the calix[4]pyrrole core undergoes a conformational change adopting the cone conformation. In this manner all four pyrrole N–H groups of the calix[4]pyrrole core can participate in hydrogen bonding interactions with the bound guest.[9]

In the cone conformation, the α,α,α,α-isomers of aryl-extended calix[4]pyrroles feature a deep aromatic cavity closed
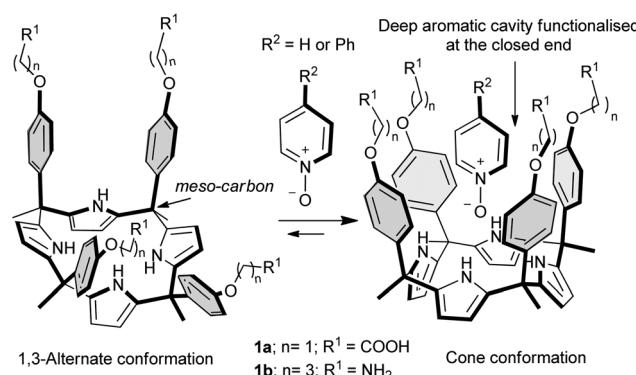


Fig. 1 The α,α,α,α-isomers of aryl-extended calix[4]pyrroles undergo a conformational change from the 1,3-alternate conformation to the cone conformation when binding with guests capable of establishing H-bonds.

at one end by four converging pyrrole NHs. The dimensions of this cavity make it suitable for the inclusion of a sizeable number of electron-rich neutral guests and anions. The included guests interact in a directed manner with the NH groups resulting in a very specific relative orientation of the binding partners. Additional weak, non-covalent interactions such as CH–π and π–π stacking can also be established between the included guests and the aromatic walls of the receptor.

The fact that aryl-extended calix[4]pyrroles possess a deep hydrophobic cavity in which the pyrrole NHs converge and are sheltered from the bulk solvent makes them very attractive for molecular recognition studies of polar guests in aqueous media. Hydrogen bonding interactions occurring in polar solvents with high dielectric constants (especially water) are frequently much weaker than those in non-polar solvents.[10,11] However, when the functional groups converge into an apolar

[a]*Institute of Chemical Research of Catalonia (ICIQ), Av. Països Catalans, 16. E-43007 Tarragona, Spain. E-mail: pballester@iciq.es*
[b]*Catalan Institution for Research and Advanced Studies (ICREA), Passeig Lluis Companys 23, E-08010 Barcelona, Spain*

cavity and are "sheltered" from the bulk water, the strength of their hydrogen bonding interactions becomes less solvent-dependent.[12–15] Indeed, enzymes take advantage of this strategy to secure vital hydrogen bonding interactions that would otherwise be washed out by competition from water molecules. While such interactions are ubiquitous in Nature, the synthesis of water soluble receptors with functional groups converging into an apolar cavity is challenging.

Recently, the rich possibilities offered by the polar and deep aromatic binding pocket of "four wall" aryl-extended calix[4]pyrroles have led to their extensive use as synthetic receptors[6,16] and binding units in supramolecular scaffolds.[17,18] These studies have been almost exclusively undertaken in organic solvents. As supramolecular chemistry develops, the understanding of molecular recognition in water, that is to say the role and the magnitude of hydrophilic and hydrophobic interactions in controlling the binding strength and selectivity, will become more and more important.[19,20]

To date, and to the best of our knowledge, only two examples of water soluble aryl-extended calix[4]pyrroles have been reported in the literature.[21,22] The example taken from the work of our group describes complexation studies in water with pyridyl N-oxides. The aryl extended calix[4]pyrroles **1** employed in the study were rendered water soluble by covalently introducing, in the *para* positions at their upper rims (*meso*-aryl groups), four ionisable groups, particularly amine and carboxylic groups. This synthetic strategy presented several design drawbacks. Firstly, the attachment of the solubilising groups to the *meso*-aryl substituents alters the electronic nature of the pristine aromatic cavity. We have previously shown that the electronic properties of the cavity are tuned by the electron-withdrawing or electron-donating character of the substituents present in the *meso*-aryl groups. Secondly and even more importantly, the presence of the solubilising groups at the upper rim impairs further elaboration of the aromatic cavity with other functional groups capable of interacting with the included guest or with other molecules providing higher order aggregates (*i.e.* dimeric capsules).

In this manuscript we report the synthesis and preliminary binding studies of a new tetraphenyl water-soluble aryl-extended calix[4]pyrrole α,α,α,α-**2** (Scheme 1). The receptor features "innocent" water-solubilising groups located at the terminus of its *meso*-alkyl substituents. The solubilising
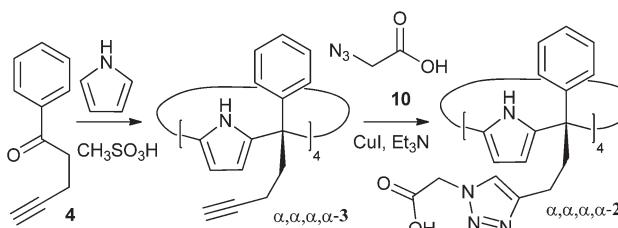
groups are sufficiently distant to avoid any interference with the pristine characteristics of the deep aromatic binding site. We envision that the described synthetic strategy will permit further elaboration of the aromatic cavity of water soluble aryl extended calix[4]pyrroles through upper rim functionalization, eventually allowing access to higher order calix[4]pyrrole-based supramolecular structures in aqueous media.

Results and discussion

Synthesis and structural characterization

The novel water-soluble aryl-extended calix[4]pyrrole α,α,α,α-**2** was synthesised in five synthetic steps. Conveniently, the ionisable water-solubilising groups are introduced in the final step. Thus, silica chromatography is an available purification technique in the synthesis of the calix[4]pyrrole precursor α,α,α,α-**3** (Scheme 2). This is an essential aspect due to the inevitable need to remove the other configurational isomers and polymeric by-products from the crude reaction mixture obtained by the condensation of butynyl phenyl ketone **4** with pyrrole.

The synthetic pathway to produce α,α,α,α-**2** requires the preliminary preparation of the butynyl phenyl ketone **4** (Scheme 2). Initially, we proceeded by alkylation of the β-keto ester **5** with propargyl bromide in the presence of DBU followed by cleavage of the ester **6** and heat promoted decarboxylation of the corresponding β-keto acid (Scheme 2, pathway a). While the alkynyl ketone **4** could be obtained through this method, the decarboxylation step turned out to be capricious. A much better and reliable synthetic route for the preparation of the butynyl phenyl ketone **4** started from acetophenone **7** and employed the methodology developed by Zaman *et al.* (Scheme 2, pathway b).[23]
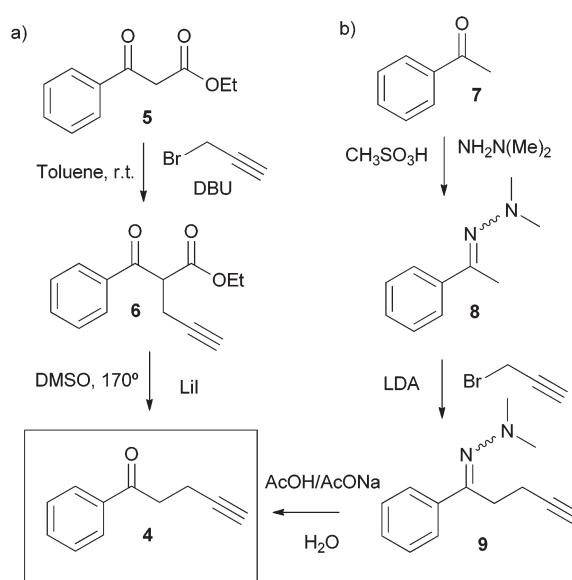
Scheme 2 Synthetic routes for the preparation of butynyl phenyl ketone **4**.

Scheme 1 Synthetic scheme for the preparation of water soluble aryl extended calix[4]pyrrole α,α,α,α-**2**.
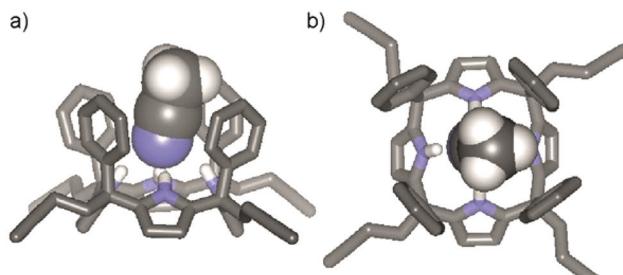
Fig. 2 (a) Side view and (b) top view of the X-ray structure of the aryl extended calix[4]pyrrole CH₃CN ⊂ α,α,α,α-**3**. For clarity, non-polar hydrogen atoms have been omitted. The included acetonitrile molecule is shown in CPK representation.

This robust synthetic pathway has the advantage of starting from simple and readily available acetophenones, meaning that water-soluble calix[4]pyrroles displaying a wide variety of *meso* aryl groups should be accessible. The acid mediated cyclocondensation of alkynyl ketone **4** and pyrrole to give α,α,α,α-**3** was very sluggish (Scheme 1). After four days, the crude reaction mixture consisted of a rich array of products, including the desired α,α,α,α-isomer of the calix[4]pyrrole **3** (Scheme 2), other configurational isomers, and higher order condensation products. Column chromatography purification of the crude mixture, followed by recrystallization with acetonitrile eventually afforded the α,α,α,α-isomer of calix[4]pyrrole **3** in low yield but with excellent purity.

The configuration of the α,α,α,α-**3** isomer was confirmed by X-ray diffraction of a single crystal that grew from the acetonitrile solution.‡ In the solid state, α,α,α,α-**3** adopts the cone conformation with a tilted molecule of acetonitrile included in its deep aromatic cavity. The nitrogen atom of the included acetonitrile is bound to the four pyrrolic NH groups, with an average N···N distance of 3.26 Å for the hydrogen bonds (Fig. 2).

Finally, the water-soluble tetracarboxylic-functionalised receptor α,α,α,α-**2** was obtained in good yield *via* 1,3 Hüisgen cycloaddition with azide **10** under standard copper(ı) catalysed conditions (Scheme 1). Gratifyingly, calix[4]pyrrole α,α,α,α-**2** is readily soluble in a variety of aqueous solutions such as diluted NaOH and, most notably, phosphate buffer saline (PBS) at pH 7.4, a solution often used to mimic biological media.

Binding studies

^{1}H NMR experiments. With the new water-soluble receptor α,α,α,α-**2** in hand, we performed a series of binding studies with three pyridine *N*-oxide derivatives (PNO) in aqueous solutions. PNO are well known to be excellent guests for calix[4]pyrroles[18,24] and have previously been shown to form highly

‡**Crystal data.** $C_{62}H_{55}N_5$, $M = 870.11$, triclinic, $a = 8.9089(3)$; $b = 14.1642(4)$; $c = 19.4386(6)$ Å, $U = 2372.83(13)$ Å³, $T = 100(2)$ K, space group: $P\bar{1}$, $Z = 2$, 18 604 reflections were measured, 10 409 unique ($R_{int} = 0.0242$) which were used in all calculations. The final $wR(F_2)$ was 0.1357 (all data). CCDC 1027046 contains the supplementary crystallographic data for this paper.
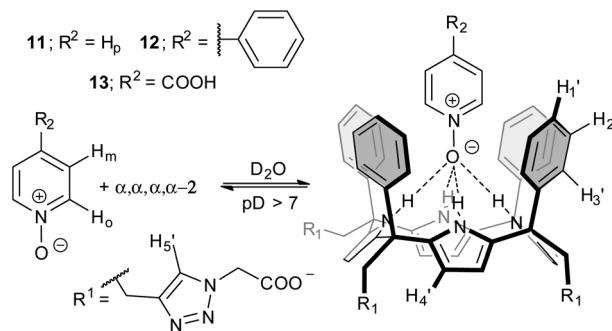
Fig. 3 Equilibrium involved in the formation of the inclusion complexes PNO ⊂ α,α,α,α-**2** and the proposed structure for the binding geometry.
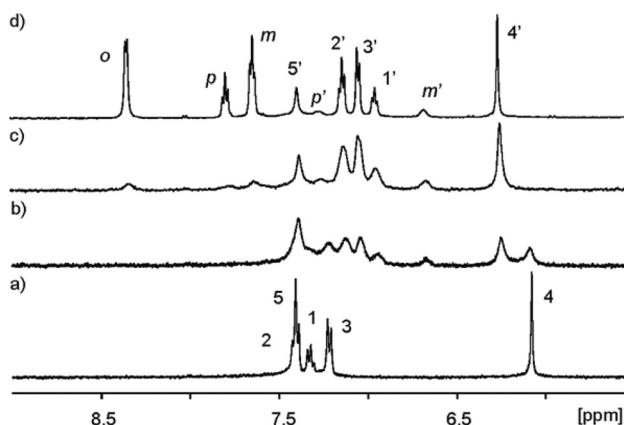
**Fig. 4** Selected downfield regions of the ^{1}H NMR spectra (400 MHz, D₂O adjusted to pD ≈ 7.6 with NaOD, 298 K) acquired during the titration of calix[4]pyrrole α,α,α,α-**2** (1 mM) with incremental amounts of **11**. (a) α,α,α,α-**2**; (b) α,α,α,α-**2** + 0.6 eq. **11**; (c) α,α,α,α-**2** + 1.1 eq. **11**; (d) α,α,α,α-**2** + 3.4 eq. **11**. Primed letters and numbers correspond to proton signals in the encapsulation complex **11** ⊂ α,α,α,α-**2**. See Fig. 3 for proton assignment and ESI† for the analogous titration with **13**.

thermodynamically and kinetically stable complexes with aryl extended calix[4]pyrroles in an aqueous solution.[21,25] Specifically, we analysed the interactions of calix[4]pyrrole α,α,α,α-**2** with pyridine *N*-oxide **11**, 4-phenylpyridine *N*-oxide **12**, and isonicotinic acid *N*-oxide **13** (Fig. 3).

Initially, we probed the interaction of calix[4]pyrrole α,α,α,α-**2** with different PNO derivatives using ^{1}H NMR spectroscopy in a basic D₂O solution (pD between 7.2 and 7.6) adjusted with NaOD. The ^{1}H NMR spectrum of α,α,α,α-**2** shows sharp signals and the characteristics of an averaged C_{4v} symmetry (Fig. 4a). The β-pyrrolic protons resonate as a singlet at $\delta = 6.1$ ppm, suggesting that the free host might adopt the cone conformation in solution.[21]

As increasing amounts of PNO **11** were added to ~1 mM aqueous solutions of α,α,α,α-**2**, the ^{1}H NMR spectra of the resulting mixtures showed that the signals corresponding to the free receptor, α,α,α,α-**2**, broadened and decreased in intensity. Concomitantly, a new set of broad signals appeared and

Fig. 5 Selected region of ROESY ^{1}H NMR spectrum of complex **11** ⊂ α,α,α,α-**2** in the presence of free **11** in excess. The cross-peaks resulting from chemical exchange between protons of free and included **11** are indicated. Primed letters correspond to signals of the protons in the complex.

grew at the expense of the signals of free α,α,α,α-**2** (Fig. 4b). This new set of signals was assigned to the protons of the calix[4]-pyrrole receptor in the 1 : 1 inclusion complex **11** ⊂ α,α,α,α-**2**. The new proton signals corresponding to the *meta* and *para* pyridyl protons of the included **11** resonating at δ ≈ 6.5 (Δδ = −0.95 ppm) and 7.1 ppm (Δδ = −0.52 ppm), respectively, also became evident. The pyridyl proton *ortho* to the nitrogen atom of **11** (not shown in Fig. 4 owing to the overlap with the broad water signal in this experiment, see Fig. 5) is the most affected by the magnetic anisotropy of the four *meso*-phenyl substituents and experiences a large upfield shift (Δδ = −4.0 ppm). This observation shows that the *N*-oxide group of bound **11** must be located at the bottom of the aromatic cavity of α,α,α,α-**2** supporting the proposed binding geometry in which the *N*-oxide forms four hydrogen bonds with the pyrrole NH.[21] When slightly more than one equivalent of **11** was added, the proton signals corresponding to the free calix disappeared (Fig. 4c). Only the proton signals of the host in the inclusion complex **11** ⊂ α,α,α,α-**2** were detected. The addition of an excess of **11** did not provoke changes in the chemical shifts of the inclusion complex but sharpened the proton signals. The proton signals corresponding to the free **11** in excess resonate as separate signals in the downfield region of the spectrum. Taken together, these results indicate that: (a) the free species and the 1 : 1 host–guest complex are involved in a chemical exchange process that is slow on the ^{1}H NMR chemical shift time scale; (b) the stability constant for the **11** ⊂ α,α,α,α-**2** can be estimated to be larger than 10^4 M$^{−1}$; and (c) the hydrogen bonded *N*-oxide **11** is rotating on its vertical axis

when included in the deep aromatic binding pocket of α,α,α,α-**2**.

The binding geometry of the **11** ⊂ α,α,α,α-**2** complex and the kinetics of the binding process were also investigated by performing a ROESY experiment on the sample containing an excess of *N*-oxide **11**.

The ROESY spectrum (Fig. 5) revealed the existence of positive cross peaks between the signals assigned to the protons of **11** in the inclusion complex and those of free **11**. This finding demonstrates that although the chemical exchange between the free and bound guest is slow on the chemical shift scale it is fast on the relaxation time scale (complex lifetime <0.1 s). The observation of a cross peak between the signal of the proton alpha to the nitrogen atom of free **11** (*ortho*, H$_o$) and the highest upfield shifted signal belonging to the protons of bound **11** confirms the location of the *N*-oxide group near the closed end of the cavity. Completely analogous results were obtained for the titration with *N*-oxide of the phenyl pyridine **12**.

The obtained results for the titration of α,α,α,α-**2** with isonicotinic acid **13** deserve a small comment (Fig. S1 and S2†). Isonicotinic acid **13**, in basic media, presents two functional groups known to bind strongly to calix[4]pyrrole units, the *N*-oxide and the carboxylate.[26,27] The inclusion of **13**, as the carboxylate, in the deep functionalised cavity of α,α,α,α-**2** produced a single set of separated proton signals for the complex **13**⁻ ⊂ α,α,α,α-**2**. The complex was formed quantitatively when 1 equiv. of **13** was added to the basic solution. The ROESY experiment performed with a solution containing the inclusion complex **13**⁻ ⊂ α,α,α,α-**2** and free **13**⁻ in excess showed that the highest upfield shifted proton of the included *N*-oxide is involved in a chemical exchange exclusively with the proton *ortho* to the nitrogen atom in the free guest. In short, the carboxylate derivative of isonicotinic **13** binds selectively through the *N*-oxide group to the α,α,α,α-**2** receptor. The carboxylate function of bound **13**⁻ is exposed to the bulk solution and its negative charge seems to have a reduced effect in the binding strength of the complex (estimated K_a(**13**⁻ ⊂ α,α,α,α-**2**) > 10^4 M$^{−1}$) when compared with those estimated for the neutral *N*-oxides.

In general, the ^{1}H NMR titration results reveal that the aryl-extended calix[4]pyrrole's hydrophobic pocket of α,α,α,α-**2** is adequate to protect the pyrrole NHs from bulk water allowing them to effectively form hydrogen bonds with pyridyl *N*-oxide guests. Although the establishment of hydrogen bonding interactions is the main factor responsible for the selectivity towards the *N*-oxide group (hydrophilic binding), the partial desolvation of the host and the guest required for the formation of the tight inclusion complexes (π–π and CH–π interactions) plays an important role in determining the binding strength (hydrophobic binding).

Isothermal titration calorimetry (ITC) experiments. The results of the ^{1}H NMR titrations were very informative to understand the geometry and stoichiometry of the inclusion complexes formed by α,α,α,α-**2** with the series of pyridyl *N*-oxides; however, their stability constants were too high to be

This journal is © The Royal Society of Chemistry 2015

Org. Biomol. Chem., 2015, **13**, 1022–1029 | **1025**

Table 1 Association constant values (K_a, M^{-1}), free energies of complexation (ΔG, kcal mol^{-1}) and corresponding enthalpic (ΔH, kcal mol^{-1}) and entropic components ($T\Delta S$, kcal mol^{-1}) measured in aqueous solution at 296 K for the inclusion complexes of the PNO series and aryl extended calix[4]pyrrole α,α,α,α-**2**

N-oxide	Medium/pH	$K_a \times 10^{4\ a}$	ΔG	ΔH^a	$T\Delta S$
11	Water/7.2^b	4.3	−6.2	−4.5	1.7
12	Water/7.2^b	20.0	−7.2	−7.4	−0.2
13	Water/7.2^b	4.5	−6.3	−6.4	−0.1

^{a} The values presented are the mean of those obtained from at least two ITC titration experiments. Errors (standard deviation) are determined to be less than 3%. ^{b} pH of water solutions was adjusted with NaOH.

Fig. 6 SCIGRESS (v 3.0.0, Fujitsu Ltd.) energy minimized (MO-G PM6 in water) structures of the inclusion complexes of the *N*-oxides with α,α,α,α-**2**: (a) **11** ⊂ α,α,α,α-**2**; (b) **12** ⊂ α,α,α,α-**2**; and (c) **13** ⊂ α,α,α,α-**2**. The *meso*-alkyl chains of the receptor were modelled as methyl groups. For clarity, only the polar hydrogen atoms of the receptor are shown and the included guest is represented as the CPK model.

measured accurately with this technique (full complex formation with 1 equiv. of *N*-oxide). For this reason, the thermodynamic characterization of the binding processes was assessed using isothermal titration calorimetry (ITC) experiments.

All the ITC titrations performed with the PNO series **11**–**13** and receptor α,α,α,α-**2** showed excellent fits to the theoretical binding isotherm for a 1 : 1 complex formation (see ESI† for titrations). The fit of the titration data to the theoretical isotherms allowed the accurate calculation of stability constant (K_a) and enthalpy (ΔH) values for the formation of the complexes. From these values, we derived the free energy of binding (ΔG) and the entropic ($T\Delta S$) component for each process. The obtained results are summarized in Table 1.

In complete agreement with the ^{1}H NMR titrations, the ITC results indicate the formation of thermodynamically highly stable complexes ($K_a > 10^4$ M^{-1}). In all cases, the binding process is mainly enthalpically driven. The entropic term is comparatively small and in the case of *N*-oxide **11** it also favours binding. These thermodynamic characteristics are in agreement with a tight fit of the interacting molecules in the complex and support the selective binding observed for the *N*-oxide group.[28]

Association constant values for the inclusion complexes of PNOs **11** and **12** with calix[4]pyrrole receptor **1a**, having four carboxy groups at the upper rim, were previously reported.[21] The reported values were measured using UV-vis titrations in H$_2$O solutions (pH = 7.2) at concentrations that were similar to those used for the ITC experiments described here. Thus, the comparison of the measured magnitudes in the two studies is reasonable. The binding constant value determined for the **11** ⊂ **1a** complex was $K_a = 1.6 \pm 0.2 \times 10^4$ M^{-1}. This value is very close to the stability constant determined in this study for the **11** ⊂ α,α,α,α-**2** complex. This indicates that moving the water solubilising anionic groups from the upper rim to the lower rim has a minimum impact on the binding of a small neutral molecule like pyridine-*N*-oxide **11** with the calix[4]pyrrole core. We foresee that the change of location of the solubilizing groups should allow the functionalization of the upper rim of the calix[4]pyrrole receptor with groups that provide higher affinity and selectivity.

In contrast with the result abovementioned, the reported binding constant for the **12** ⊂ **1a** ($K_a = 2.4 \pm 1.3 \times 10^3$ M^{-1}) was two orders of magnitude smaller than the one measured in this study for the related **12** ⊂ α,α,α,α-**2** complex. This result indicated that the location of the water solubilising groups at the lower rim of a calix[4]pyrrole scaffold had a positive effect in the binding of larger *N*-oxides like **12**. In this case, the use of the alternative synthetic methodology for the placement of the solubilising groups at the lower rim without further modification of the upper rim was rewarding.

Interestingly, the binding constant values determined for PNOs **11** and [**13**]$^-$ with receptor α,α,α,α-**2** are almost identical. This surprised us, as we expected the negatively charged [**13**]$^-$ *N*-oxide to form a thermodynamically weaker complex with the also negatively charged, in basified water, calix[4]pyrrole α,α,α,α-**2**.§ In water, the strong repulsive electrostatic interactions established between negative charges are highly attenuated, allowing the two molecules to form a tight complex.

Not surprisingly, however, the thermodynamic characteristics of the two binding processes are indeed significantly different. Meanwhile, the stability constant for the complex formed between phenyl-substituted *N*-oxide **12** and receptor α,α,α,α-**2** is almost five-fold larger than that of *N*-oxide **11**. At first sight, this result could be attributed to the higher hydrophobicity of phenyl pyridyl *N*-oxide **12** with respect to pyridyl *N*-oxide **11**. Larger apolar aromatic surfaces translate into higher hydrophobicity and a stronger hydrophobic effect because of the favourable increase in desolvation entropy. However, in the case at hand, the enhanced binding of **12** with respect to **11**, results from an enthalpic gain on complex formation. In addition, the contacts in the surface area for complexes **12** ⊂ α,α,α,α-**2** and **11** ⊂ α,α,α,α-**2** are predicted to be similar, only the end of the pyridyl *N*-oxide residue is included in the binding site (Fig. 6). The thermodynamic characteristics suggest a tighter geometry for the **12** ⊂ α,α,α,α-**2** complex that,

§ The protonation constants for the receptor α,α,α,α-**2** were not determined, but in analogy to compound **1a**, it is expected that in water solution at pH = 7.2 the former will be exclusively presented as a tetraanionic species.

as expected, is accompanied by a reduction in entropy gain, when compared to the looser complex formed with **11**.

Conclusion

In conclusion, we have described the synthesis of a novel water-soluble aryl-extended calix[4]pyrrole α,α,α,α-**2**. In contrast to previous examples, the water-solubilising groups are distal to the binding site. This leaves the binding site and the upper rim of the calix[4]pyrrole pristine, making possible the future functionalization of the *meso*-aryl rings, thus, permitting the construction of more complicated calix[4]pyrroles. The receptor α,α,α,α-**2** forms thermodynamically and kinetically stable complexes with a series of pyridyl *N*-oxide guests in aqueous solution. The binding geometry of these complexes was probed using ^{1}H NMR titrations and their thermodynamic characteristics were determined using ITC experiments. The obtained results also demonstrated that calix[4]pyrrole α,α,α,α-**2** preferentially engages in hydrogen bonding interactions of the four pyrrole NHs with a *N*-oxide moiety than with a carboxylate group. Nevertheless, the anionic α,α,α,α-**2** receptor binds negatively charged pyridyl *N*-oxides with high affinity. Our results showcase the ability of the receptor's aromatic pocket to protect the pyrrole N–H groups and ensure selective hydrogen-bonding interactions even in water.

Experimental

General

Reagents were obtained from commercial suppliers and used without further purification. All solvents were commercially obtained and used without further purification except for pyrrole which was distilled (50 mbar, 58–59 °C) and then stored in the freezer for further use. Where indicated, solvents were degassed by 3 freeze–pump–thaw cycles. Routine ^{1}H NMR and ^{13}C NMR spectra were recorded on a Bruker Avance 300 (300 MHz for ^{1}H NMR), Bruker Avance 400 (400 MHz for ^{1}H NMR), Bruker Avance 500 (500 MHz for ^{1}H NMR) ultrashield spectrometer, or on a Bruker Avance III 500 (500 MHz for ^{1}H NMR) with a QNP cryoprobe. The deuterated solvents (Aldrich) used are indicated in the Experimental section; chemical shifts are given in ppm. For CDCl$_3$ the peaks were referenced relative to the solvent residual peak δ_H = 7.26 ppm and δ_C = 77.0 ppm. For D$_2$O the peaks were referenced relative to the solvent residual peak δ_H = 4.79 ppm. All NMR *J* values are given in Hz. High resolution mass spectra were obtained on a MicroTOF II (Bruker Daltonics) ESI as ionization mode Mass Spectrometer or on a Bruker Ultraflex MALDI-TOF-TOF Mass spectrometer. Column chromatography was performed with silica gel, technical grade, pore size 60 Å, and 230–400 mesh particle size. Crystal structure determination was carried out using a Bruker-Nonius diffractometer equipped with an APEX 2 4K CCD area detector, a FR591 rotating anode with MoKα

radiation, Montel mirrors as the monochromator and a Kryoflex low temperature device (*T* = 100 K). Full sphere data collection was carried out by omega and phi scans. Programs used: data collection Apex2 V. 1.0–22 (Bruker-Nonius 2004), data reduction Saint + Version 6.22 (Bruker-Nonius 2001) and absorption correction SADABS V. 2.10 (2003). Crystal structure solution was achieved using direct methods as implemented in SHELXTL Version 6.10 (Sheldrick, Universität Göttingen (Germany), 2000) and visualized using the XP program. Missing atoms were subsequently located from difference Fourier synthesis and added to the atom list. Least-squares refinement on F^2 using all measured intensities was carried out using the program SHELXTL Version 6.10 (Sheldrick, Universität Göttingen (Germany), 2000).

Procedures and characterisation data

Synthesis of butynyl phenyl ketone 4. The synthesis of the ketone involves two steps: *Step 1, hydrazone formation.*[29] Benzene (38.5 mL) was added to acetophenone (7 mL, 59.4 mmol, 1 equiv.) contained in a 100 mL round bottom flask equipped with a Dean-Stark apparatus and under an argon atmosphere. Then 1,1-dimethylhydrazine (13.3 mL, 171 mmol, 3 equiv.) was added followed by methanesulfonic acid (0.19 mL, 2.93 mmol, 5 mol%). After the addition of the acid, the mixture turned yellow. The reaction was subjected to reflux overnight, during which time water collected in the Dean-Stark trap. The next day the reaction mixture was concentrated under reduced pressure, affording the crude hydrazone **8** as a light yellow oil with a small amount of solid 10.5 g. This material was distilled at reduced pressure (13 mbar). The desired hydrazone **8** distilled in the range of 98–105 °C as a light yellow oil (8.5 g 88%). The ^{1}H NMR spectrum is in agreement with that previously reported in the literature.[30]

Step 2 alkylation and hydrolysis of the hydrazone.[23] Lithium diisopropylamide (6.29 mL, 1.96 M, 12.33 mmol, 2 equiv.), freshly titrated using diphenylacetic acid as an indicator, was added to a solution at −74 °C (achieved using a dry ice/acetone bath) of hydrazine **8** (1 g, 6.16 mmol, 1 equiv.) in THF (15 mL, freshly distilled from sodium benzophenone) under an argon atmosphere. After 1 hour, 3-bromoprop-1-yne (80% solution in toluene, 0.69 mL, 6.16 mmol, 1 equiv.) was added dropwise *via* a syringe. The reaction was stirred overnight while coming to RT. The next day, the reaction was quenched by adding 40 mL of saturated NH$_4$Cl$_{(aq)}$. The reaction mixture was extracted with diethylether (3 × 20 mL) and the organic extracts were combined, dried over Na$_2$SO$_4$, filtered and concentrated under vacuum to give a brown residue. Acetic acid 3 mL, sodium acetate 1.45 g, water 0.5 mL and THF 3 mL were added to the resulting residue and the reaction was stirred under air until complete hydrolysis of the hydrazone was observed by ^{1}H NMR (typically 7 hours). The reaction mixture was quenched by adding NaOH$_{(aq)}$ (2 M) at 0 °C until the pH of the mixture was basic as judged by litmus paper. The mixture was stirred for 20 min and then 20 mL of diethyl ether were added. The two phases were separated and the aqueous layer was extracted with diethyl ether (2 × 20 mL). The organic extracts were

combined, washed with 50 mL of water, and then with 50 mL of brine. Finally the organic extract was dried over Na_2SO_4, filtered and concentrated under vacuum, affording 0.82 g of the crude product as a black solid. The solid was purified by column chromatography (40 g SiO_2 column, 1 : 1 DCM–hexane eluent, product RF = 0.5). The ketone 4 was obtained as light yellow crystals which were then sublimed in a bulb to bulb apparatus (0.1 mmHg, 80 °C), affording a white microcrystalline powder (0.63 g, 65%).The ^1H NMR spectrum is in agreement with that previously reported in the literature.[31]

Synthesis of calixpyrrole 3. Degassed methanol (10 mL) was added to pyrrole (0.44 mL, 6.34 mmol, 1 equiv.) and methanesulphonic acid (1.23 mL, 18.95 mmol, 3 equiv.) contained in a 50 mL round bottom flask under an argon atmosphere. Next, a methanolic solution of ketone 4 (17 mL, 0.37 M, 6.32 mmol, 1 equiv.) was added *via* a syringe to the reaction mixture (a little bit of heat is necessary to completely dissolve the ketone). After 4 days of stirring at room temperature, the reaction mixture was neutralized by adding 80 mL of saturated $NaHCO_{3(aq)}$. The mixture was extracted with DCM (3 × 50 mL). The DCM extracts were combined, dried over Na_2SO_4 filtered, and concentrated under vacuum, affording 0.7 g of a dark colored residue. The crude was purified by column chromatography (20 g SiO_2, DCM–hexane 65 : 35, product RF = 0.4). Two separate fractions containing the product were isolated: the first fraction (11.6 mg) contained the desired product and other configurational isomers. The second fraction (78 mg) contained the α,α,α,α-3 isomer and an unidentified impurity with similar RF = 0.4. Both fractions were separately dissolved in a minimum of hot acetonitrile. The solutions were cooled at 0 °C and the α,α,α,α-3 isomer crystalized as small colorless cubes, 21.9 mg, >1% yield. ^1H NMR (300 MHz, $CDCl_3$, 25 °C): δ (ppm) 7.25 (bs, 4H), 7.18–7.07 (m, 20H), 5.92 (d, J = 2.7 Hz, 8H), 2.56 (m, 8H), 2.09 (m, 8H), 1.95 (t, J = 2.6 Hz, 4H); $^{13}C\{^1H\}$ NMR (125 MHz, $CDCl_3$ 25 °C): δ (ppm) 135.1, 128.2, 128.1, 127.0, 106.4, 100.2, 84.5, 68.6, 48.6, 39.3, 15.0; HRMS (ESI-TOF) *m/z*: [M + Na]$^+$ calcd for $C_{60}H_{53}N_4$ 829.4265; Found 829.4282; IR $\tilde{v}$ (cm^{-1}) 2116, 2961, 3301, 3370, 3404; m.p. 214–224 °C decomposition.

Synthesis of 2-azidoacetic acid 10.[32] Dry DMF (15 mL) was added to methyl bromoacetate (8 mL, 87 mmol, 1 equiv.) contained in a 100 mL round-bottom flask under an argon atmosphere. The solution was stirred vigorously while sodium azide (6.21 g, 95 mmol, 1.1 equiv.) was added in several small portions. The reaction mixture was stirred for an additional 2.5 hours followed by the addition of 50 mL of distilled water. The reaction mixture was extracted with diethyl ether (2 × 50 mL). Evaporation of the solvent afforded a light yellow oil. The oil was dissolved in 40 mL of THF and 40 mL of water. While stirring, 3 g of KOH were added to the solution in small portions. The mixture was stirred for 2.5 hours at 40 °C, cooled at r.t. and washed with ethyl acetate (50 mL). The aqueous layer was acidified with HCl (1 M) until the pH of the solution was roughly 1 as judged by litmus paper. The aqueous layer was extracted with ethyl acetate (2 × 50 mL). Evaporation of the solvent afforded the product 10 as a colorless oil (3.85 g, 44%

yield). The ^1H NMR spectrum is in agreement with that previously reported in the literature.[32]

Synthesis of calixpyrrole α,α,α,α-2 isomer. Degassed DMSO (0.9 mL) was added to α,α,α,α-calixpyrrole 3 (10 mg, 12 μmol, 1 equiv.) and 2-azidoacetic acid 10 (19 mg, 0.19 mmol, 16 equiv.) contained in a 2 mL flask under an argon atmosphere. Then, CuI (9.2 mg, 48 μmol) was added followed by Et_3N (7.9 mg, 77 μmol). A precipitate was immediately formed. The mixture was stirred vigorously and after 1 h the reaction was complete as judged by TLC. The reaction mixture was diluted with water (30 mL) and 10% $HCl_{(aq)}$ (10 mL) inducing the appearance of a solid that was isolated by filtration. The solid was washed with water (3 mL). Acetone was added to dissolve the filtered solid. The acetone solution was evaporated under vacuum to give 9.8 mg of the α,α,α,α-2 isomer as a white powder, 66% yield. ^1H NMR (400 MHz, D_2O pD adjusted to 8 with NaOD, 25 °C): δ (ppm) 7.41 (m, 12H), 7.33 (m, 4H), 7.22 (d, J = 7.63 Hz, 8H), 6.08 (s, 8H), 4.89 (s, 8H), 2.82 (m, 8H), 2.48 (m, 8H); $^{13}C\{^1H\}$ NMR (125 MHz cryoprobe, D_2O pD adjusted to 8 with NaOD, 25 °C): δ (ppm) 174.7, 149.3, 145.7, 138.7, 129.9, 129.8, 128.5, 125.2, 106.9, 54.5, 49.9, 39.4, 22.4. HRMS (MALDI-TOF) *m/z*: [M + Na]$^+$ calcd for $C_{68}H_{64}N_{16}NaO_8$ 1255.4985; Found 1255.4998, IR $\tilde{v}$ (cm^{-1}) 1728, 3332; m.p. 190 °C (decomposition).

Acknowledgements

Notes and references

1 P. A. Gale, J. L. Sessler and V. Kral, *Chem. Commun.*, 1998, 1–8.

2 P. A. Gale, P. Anzenbacher and J. L. Sessler, *Coord. Chem. Rev.*, 2001, **222**, 57–102.

3 J. L. Sessler, D. E. Gross, W. S. Cho, V. M. Lynch, F. P. Schmidtchen, G. W. Bates, M. E. Light and P. A. Gale, *J. Am. Chem. Soc.*, 2006, **128**, 12281–12288.

4 S. K. Kim and J. L. Sessler, *Acc. Chem. Res.*, 2014, **47**, 2525–2536.

5 W. E. Allen, P. A. Gale, C. T. Brown, V. M. Lynch and J. L. Sessler, *J. Am. Chem. Soc.*, 1996, **118**, 12471–12472.

6 P. Anzenbacher, K. Jursíková, V. M. Lynch, P. A. Gale and J. L. Sessler, *J. Am. Chem. Soc.*, 1999, **121**, 11020–11021.

7 L. Bonomo, E. Solari, G. Toraman, R. Scopelliti, M. Latronico and C. Floriani, *Chem. Commun.*, 1999, 2413–2414.

8 J. R. Blas, J. M. Lopez-Bes, M. Marquez, J. L. Sessler, F. J. Luque and M. Orozco, *Chem. – Eur. J.*, 2007, **13**, 1108–1116.

1028 | *Org. Biomol. Chem.*, 2015, **13**, 1022–1029

This journal is © The Royal Society of Chemistry 2015

9 Y. D. Wu, D. F. Wang and J. L. Sessler, *J. Org. Chem.*, 2001, **66**, 3739–3746.

10 C. Allott, H. Adams, P. L. Bernad, C. A. Hunter, C. Rotger and J. A. Thomas, *Chem. Commun.*, 1998, 2449–2450.

11 V. M. Rotello, E. A. Viani, G. Deslongchamps, B. A. Murray and J. Rebek, *J. Am. Chem. Soc.*, 1993, **115**, 797–798.

12 B. Sookcharoenpinyo, E. Klein, Y. Ferrand, D. B. Walker, P. R. Brotherhood, C. F. Ke, M. P. Crump and A. P. Davis, *Angew. Chem., Int. Ed.*, 2012, **51**, 4586–4590.

13 M. Torneiro and W. C. Still, *J. Am. Chem. Soc.*, 1995, **117**, 5887–5888.

14 J. D. Howgego, C. P. Butts, M. P. Crump and A. P. Davis, *Chem. Commun.*, 2013, **49**, 3110–3112.

15 G. Joshi and A. P. Davis, *Org. Biomol. Chem.*, 2012, **10**, 5760–5763.

16 G. Gil-Ramírez, E. C. Escudero-Adán, J. Benet-Buchholz and P. Ballester, *Angew. Chem., Int. Ed.*, 2008, **47**, 4114–4118.

17 M. Chas and P. Ballester, *Chem. Sci.*, 2012, **3**, 186–191.

18 M. Espelt and P. Ballester, *Org. Lett.*, 2012, **14**, 5708–5711.

19 E. A. Kataev and C. Muller, *Tetrahedron*, 2014, **70**, 137–167.

20 G. V. Oshovsky, D. N. Reinhoudt and W. Verboom, *Angew. Chem., Int. Ed.*, 2007, **46**, 2366–2393.

21 B. Verdejo, G. Gil-Ramírez and P. Ballester, *J. Am. Chem. Soc.*, 2009, **131**, 3178–3179.

22 K. D. Bhatt, D. J. Vyas, B. A. Makwana, S. M. Darjee and V. K. Jain, *Spectrochim. Acta, Part A*, 2014, **121**, 94–100.

23 S. Zaman, M. Kitamura and A. D. Abell, *Aust. J. Chem.*, 2007, **60**, 624–626.

24 L. Adriaenssens and P. Ballester, *Chem. Soc. Rev.*, 2013, **42**, 3261–3277.

25 L. Adriaenssens, J. L. Acero Sanchez, X. Barril, C. O'Sullivan and P. Ballester, *Chem. Sci.*, 2014, **5**, 4210–4215.

26 D. E. Gross, D. W. Yoon, V. M. Lynch, C. H. Lee and J. L. Sessler, *J. Inclusion Phenom. Macrocyclic Chem.*, 2010, **66**, 81–85.

27 J. Kříž, J. Dybal, E. Makrlík, Z. Sedláková and V. Kašička, *Chem. Phys. Lett.*, 2013, **561–562**, 42–45.

28 Highly selective substrate binding should be enthalpically driven see: F. Diederich, *Cyclophanes*, The Royal Society of Chemistry, Cambridge, 1991.

29 H. F. Motiwala, B. Gülgeze and J. Aubé, *J. Org. Chem.*, 2012, **77**, 7005–7022.

30 S. D. Sharma and S. B. Pandhi, *J. Org. Chem.*, 1990, **55**, 2196–2200.

31 H. Imagawa, T. Kurisaki and M. Nishizawa, *Org. Lett.*, 2004, **6**, 3679–3681.

32 C. K. Y. Chun and R. J. Payne, *Aust. J. Chem.*, 2009, **62**, 1339–1343.

This journal is © The Royal Society of Chemistry 2015

Org. Biomol. Chem., 2015, **13**, 1022–1029 | **1029**